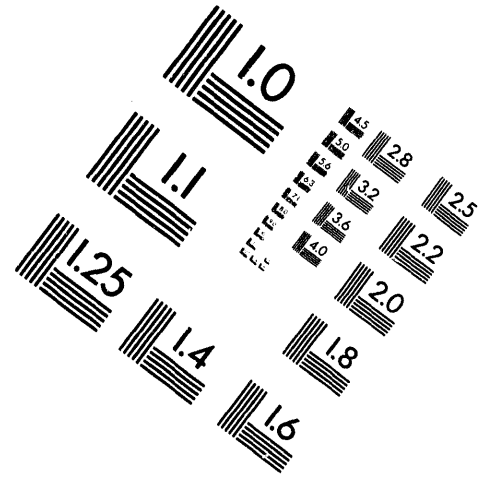
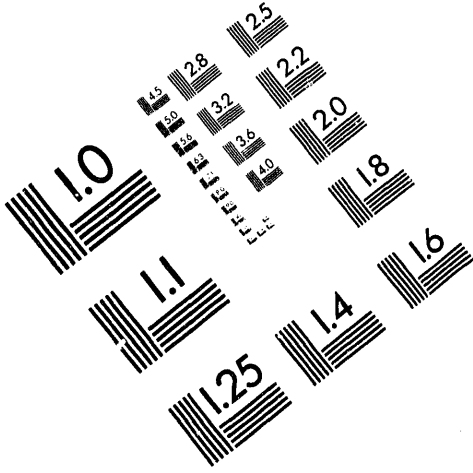




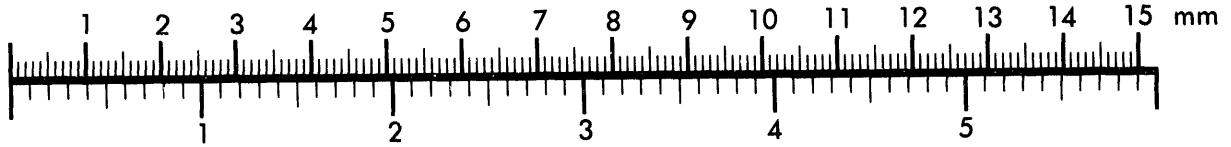
**AIM**

**Association for Information and Image Management**

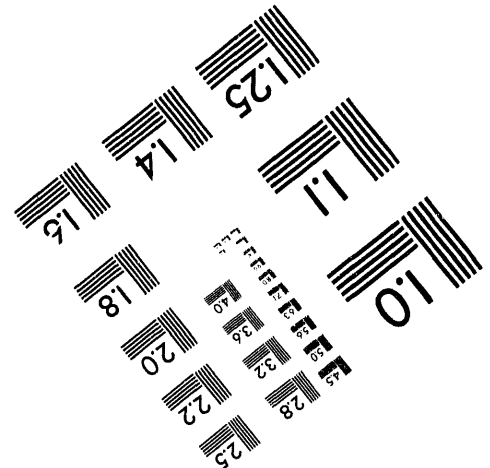
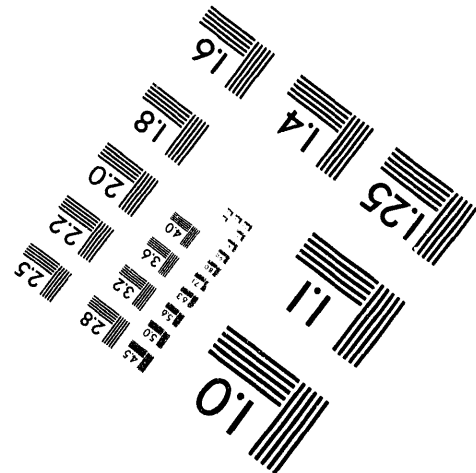
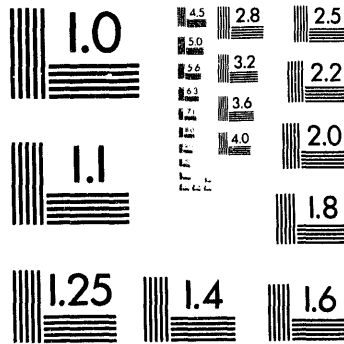
1100 Wayne Avenue, Suite 1100  
Silver Spring, Maryland 20910  
301/587-8202



Centimeter



Inches



MANUFACTURED TO AIM STANDARDS  
BY APPLIED IMAGE, INC.

**1 of 1**

## CHARGED PARTICLE DYNAMICS IN THE ACCELERATION GAP OF THE PBFA II ION DIODE

J. E. Bailey, A. L. Carlson, A. B. Filuk, D. J. Johnson, P. Lake,  
E. J. McGuire, T. A. Mehlhorn, T. D. Pointon, and T. J. Renk  
Sandia National Laboratories, P.O. Box 5800, Albuquerque NM, 87185-1187  
and  
Y. Maron  
Weizmann Institute of Science, Rehovot 76100, Israel

### Abstract

*We are improving the understanding of pulsed-power-driven ion diodes using measurements of the charged particle distributions in the diode anode-cathode (AK) gap. We measure the time- and space-resolved electric field in the AK gap using Stark-shifted Li I 2s-2p emission. The ion density in the gap is determined from the electric field profile and the ion current density. The electron density is inferred by subtracting the net charge density, obtained from the derivative of the electric field profile, from the ion density. The measured electric field and charged particle distributions are compared with results from QUICKSILVER, a 3D particle-in-cell computer code. The comparison validates the fundamental concept of electron build-up in the AK gap. However, the PBFA II diode exhibits considerably richer physics than presently contained in the simulation, suggesting improvements both to the experiments and to our understanding of ion diode physics.*

The ion current accelerated using an applied-B ion diode is primarily determined by the voltage and the charged particle distribution in the anode-cathode (AK) gap. We are improving the understanding of ion diode physics by measuring the charged particle distributions in the AK gap of the cylindrically-symmetric Applied-B ion diode on the PBFA II accelerator [1]. This diode generates a 15-25 nsec,  $\sim 10$  MeV, 6-9 TW lithium ion beam, accelerated across a typically 18 mm AK gap [2]. A schematic of the diode is shown in Figure 1 and typical voltage and current waveforms are shown in Figure 2. The gap is insulated against electron current by the application of a 2-3 T magnetic field along the symmetry axis. During the pulse, electrons accumulate in the AK gap both by injection from the transmission line feeding the diode and from the cathode tips. The enhancement of the ion current above the Child-Langmuir space-charge limit is controlled by the number and radial distribution of these electrons across the AK gap. The charged particle distribution also affects the beam divergence, since non-radial electric fields can be generated either by

instabilities or non-uniformities in the charged particle cloud. Our goal is to achieve an experimentally-validated understanding of the charged particle distributions that will lead to improved ion beam power.

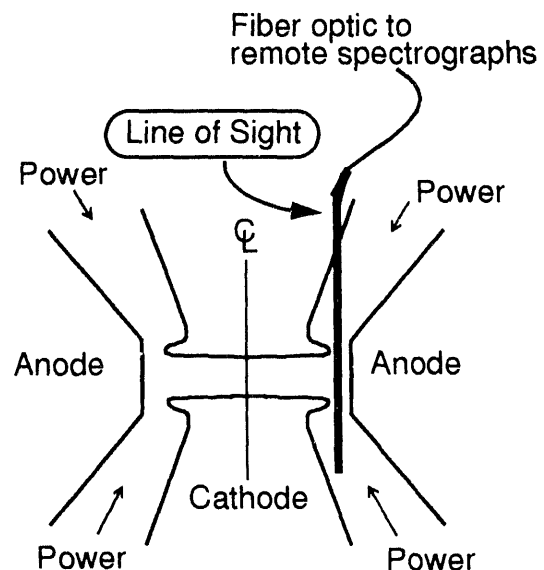


Figure 1. Schematic of PBFA II diode.

**MASTER**

DISTRIBUTION OF THIS DOCUMENT IS UNLIMITED

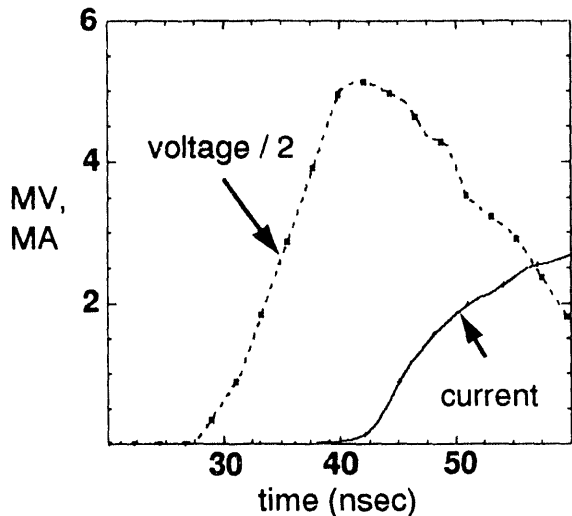


Figure 2. Voltage and current waveforms measured on PBFA II shot 6408.

Time- and space-resolved visible spectroscopy of emission from lithium neutrals in the AK gap is the primary diagnostic in this effort [3]. Fiber optics transport light collected from the diode to a remote screen room, where it is recorded using a novel streak camera/spectrograph configuration [4]. The diagnostic system simultaneously provides  $\sim 1$  nsec time resolution,  $\sim 1$  Å spectral resolution, and 2 mm spatial resolution, with 11 independently-aimed lines of sight presently available. The spatial resolution can be increased at the cost of lower collected light. A typical configuration is five lines of sight located at different radii in one azimuth and six lines of sight located at different radii in another azimuth  $180^\circ$  away. This enables us to measure both radial and azimuthal variations as a function of time in a single shot.

We investigate the AK gap dynamics using the Stark-shifted Li I 2s-2p line to measure the evolution of the electric field profile. Two independent calculations of the Stark pattern under crossed electric and magnetic fields were performed to ensure reliability. The field near the anode is typically  $\sim 10$  MV/cm, the highest ever directly measured with the Stark effect. Measurements of the electric field  $E$  enable us to determine the charged particle distribution [5] from  $\nabla \cdot E = 4\pi\rho = e(Zn_i - n_e)$ , where  $\rho$  is the net charge density,  $e$  is the elec-

tron charge, and  $n_e$ ,  $n_i$  are the electron and ion densities, respectively. Assuming that the electric field is predominantly radial, the ion velocity is given by integrating the field radially-inward from the anode, using  $v_i^2 = 2Ze/m_i \int E_r dr$ . Knowing the local ion velocity, we can determine the ion density from  $n_i = J_i/(Zev_i)$ , where  $J_i$  is the ion current density measured with Faraday cups or a magnetic spectrograph. The electron density  $n_e$  is obtained by subtracting the net charge density from the ion density times the ion charge. The result is a time- and space-resolved determination of  $n_e$  and  $n_i$  in the AK gap.

We evaluate our present understanding of ion diode physics by comparing the measured PBFA II electric field distribution and charged particle densities with results from QUICKSILVER [6], a three-dimensional fully-electromagnetic particle-in-cell computer code. This code uses the applied accelerator power pulse and realistic magnetic field geometries to calculate the ion and electron distributions self-consistently, including the effects of field fluctuations due to instabilities.

The electric field profile evolution on PBFA II shot #6408 with corresponding simulation results is shown in Figure 3. This shot used a 10 cm tall flat anode, an 18 mm AK gap, and a 17.5 MV  $V_{crit}$ , where  $V_{crit}$  quantifies the insulating magnetic flux in the AK gap as the electron

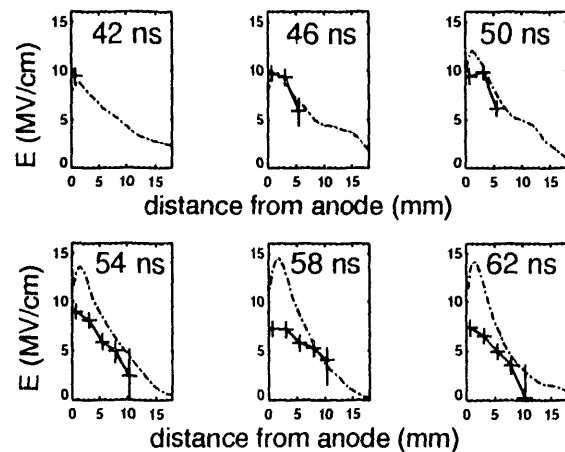


Figure 3. Electric field evolution on PBFA II shot 6408 compared to simulation. Crosses are data and solid line is simulation.

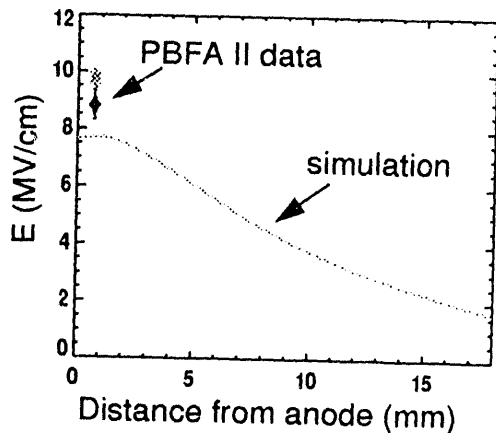


Figure 4. Data from PBFA II shot 6408 and simulation result, both corresponding to the onset of ion current (38 ns, see Figure 2).

energy needed to cross the gap. Each plot represents an average over 4 nsec with an inter-plot spacing of 4 nsec. The error bars on this and subsequent plots represent one standard deviation. Qualitatively, the simulation fidelity is very reasonable early in the pulse, especially considering the complexity of the physics. However, there are clear discrepancies later in time, affecting predictions of divergence and power coupling. These discrepancies arise at the onset of non-uniform ion emission and a parasitic loss current in the experiments, which are not currently modeled in the simulations.

Typical data and simulation results corresponding to the onset of ion current are shown in Figure 4. The  $\sim 10$  MV diode voltage across the 1.8 cm physical AK gap with  $\sim 9$  MV/cm electric field near the anode at the onset of the ion current implies that the electron density in the diode is high enough to modify the field profile even at this early time. The initial field profile is also modified by electrons in the simulation, but the field value is somewhat lower, indicating fewer electrons in the gap. The simulations suggest that the high electron density in the gap early in time is primarily due to injection of electrons from the MITL.

The electric field measured near the anode surface remains high throughout most of the pulse (Figure 3). This observation is contrary to the expectation that the electric field for a space-charge-limited source should vanish at the anode. Figure 5 shows a comparison of the PBFA II elec-

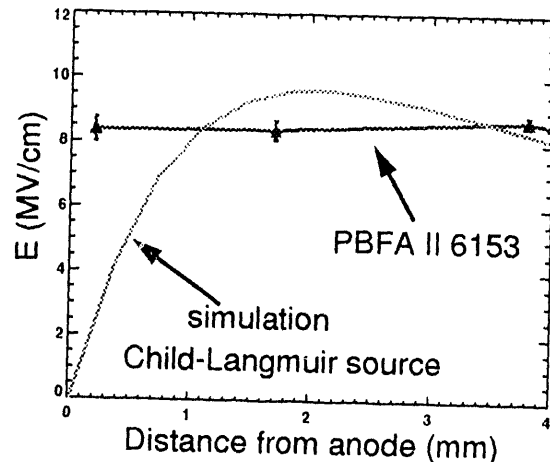


Figure 5. Electric field near the anode from PBFA II shot 6153, and a corresponding simulation that assumed a space-charge-limited source.

tric field in the vicinity of the anode with a simulation that assumed a space-charge-limited source (all other simulations shown here assumed a field threshold of 7 or 9 MV/cm for ion emission). The data are consistent with a recent theory [7] that suggests the LiF ion source operates as an electron-deposition-assisted, field-limited ion emitter. The 7-9 MV/cm ion emission field we observe is also consistent with some electron filling of the diode prior to ion current initiation, in order to increase the  $\sim 5$  MV/cm vacuum-gap field. Work is in progress to evaluate the impact of this field-limited emission effect on the diode power coupling.

Three other new diode phenomena have been observed in these experiments. First, over much of the pulse the net charge density is approximately zero near the PBFA II anode (Figure 6), implying that the electron density increases near the anode. This is in contrast to the simulations, which have a well-defined separation between the anode and the electrons. It should be noted that in the simulations there is no source of electrons at or near the anode. Second, strong azimuthal non-uniformities in electric field, and thus also in the charged particle densities, exist in the experiment (Figure 7). These non-uniformities persist over 10-30 nsec time-scales, despite the expectation that azimuthally drifting electrons should cancel such asymmetries in  $\sim 5$  nsec. Third, the sign of  $dE/dr$  changes from negative to positive near the middle of the PBFA II gap (Figure 8), signifying that the

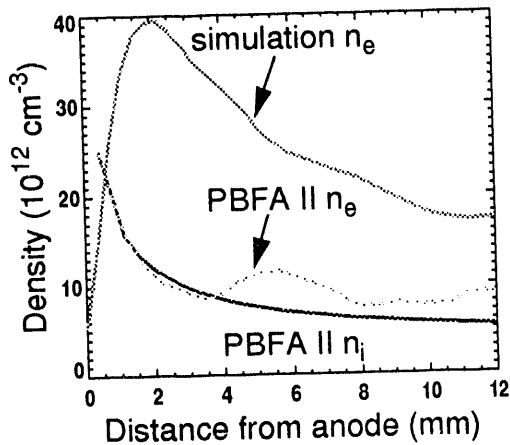


Figure 6. Electron and ion densities corresponding to the PBFA II electric field profile shown in Figure 5. Simulation assumed a 7 MV/cm threshold field for ion emission. Note simulation  $n_e$  is much larger than PBFA II  $n_e$  overall because of larger simulation ion current at this time.

local ion density exceeds the electron density. This indicates either a sudden loss of electrons or local surplus of ions.

The spectroscopic measurements in the diode acceleration gap provide information with a level of detail that was previously unattainable in high-power diodes, since only measurements of the accelerated ion beam properties were available. Some of the newly-discovered diode phenomena,

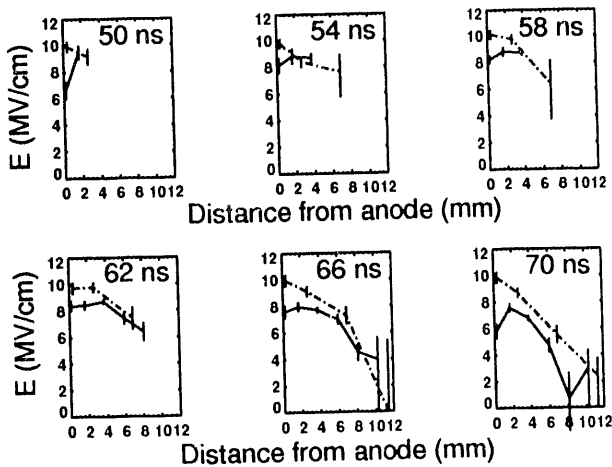


Figure 7. Electric field evolution on PBFA II shot 6153, measured in two azimuths separated by 180°. Ion current onset is at 46 nsec. The solid line is for one azimuth, the dashed line is for the other.

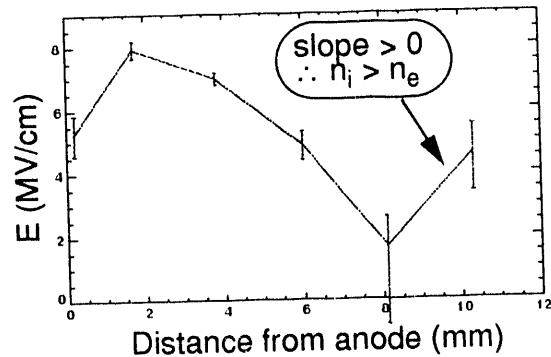


Figure 8. Electric field from PBFA II 6153 at  $t = 70$  nsec.

such as azimuthal asymmetries, are probably best addressed by seeking to eliminate them from the experiments. This alone could be highly beneficial, since eliminating asymmetries may improve the diode impedance and beam divergence. However, our understanding of diode behavior must also be revised and expanded to incorporate this new information. The differences between the idealized diode simulated by QUICKSILVER and the actual PBFA II diode reflect this need. The results show that although the actual diode behavior is more complex than in our diode simulations, we now have a method for improving and experimentally validating our understanding of diode physics.

This work performed by Sandia National Laboratories, supported by the U.S. Department of Energy under contract DE-AC04-94AL85000.

- <sup>1</sup> D.J. Johnson et. al., *Proc. 7th IEEE Pulsed Power Conf., Monterey, CA.*, ed. by R. White and B.H. Bernstein, p. 944 (1989).
- <sup>2</sup> T.A. Mehlhorn et. al., these proceedings.
- <sup>3</sup> J.E. Bailey, A.L. Carlson, R.L. Morrison, and Y. Maron, *Rev. Sci. Instr.* **61**, 3075 (1990).
- <sup>4</sup> J.E. Bailey, A.L. Carlson, and P. Lake, *1994 IEEE Int. Conf. on Plasma Science, Santa Fe, N.M.* (Catalog #94CH3465-2), p. 133.
- <sup>5</sup> Y. Maron, M.D. Coleman, D.A. Hammer, and H.S. Peng, *Phys. Rev. Lett.* **57**, 699 (1986) and *Phys. Rev.* **A36**, 2818 (1987).
- <sup>6</sup> D.B. Seidel, M.L. Kiefer, R.S. Coats, T.D. Pointon, J.P. Quintenz, and W.A. Johnson, in *Computational Physics*, ed. by A. Tenner (World Scientific, Singapore, 1991), p. 475.
- <sup>7</sup> T. Green, private communication, 1993.

### **DISCLAIMER**

This report was prepared as an account of work sponsored by an agency of the United States Government. Neither the United States Government nor any agency thereof, nor any of their employees, makes any warranty, express or implied, or assumes any legal liability or responsibility for the accuracy, completeness, or usefulness of any information, apparatus, product, or process disclosed, or represents that its use would not infringe privately owned rights. Reference herein to any specific commercial product, process, or service by trade name, trademark, manufacturer, or otherwise does not necessarily constitute or imply its endorsement, recommendation, or favoring by the United States Government or any agency thereof. The views and opinions of authors expressed herein do not necessarily state or reflect those of the United States Government or any agency thereof.

**DATE**

**FILMED**

*10 / 3 / 94*

**END**



